

ScienceDirect

Procedia CIRP 00 (2022) 000-000



12th CIRP Conference on Photonic Technologies [LANE 2022], 4-8 September 2022, Fürth, Germany

Numerical modeling and simulation of ultrafast laser-matter interaction with aluminum thin film

Shuting Lei^{a*}, Xinya Wang^a and Jon T. Larsen^b

^aKansas State University, 1701D Platt St, Manhattan, KS 66506, USA ^bCascade Applied Sciences Inc, 6325 Trevarton Dr, Longmont, CO 80503, USA

* Corresponding author. Tel.: +1-785-323-7498; fax: +1-785-532-3738. E-mail address: lei@ksu.edu

Abstract

Modeling and simulation of laser-matter interaction with aluminum thin film on silicon substrate is conducted using a 1D radiation hydrodynamics code, known as HYADES. Various physical processes at the microscopic/atomic level during laser-matter interaction including laser deposition, ionization, thermal energy transport, and hydrodynamics motion are considered in the model. To validate the numerical model, single pulse laser irradiation experiments are conducted. Cross sectional profiles of the ablation sites are characterized, and ablation depths are extracted from the profiles. The numerical model is verified by comparing model predictions with experimental results. The validated model will be used in the future to study the effects of various laser parameters (e.g., laser fluence, pulse duration, laser wavelength, pulse train) on ablation efficiency and quality (e.g., ablation depth, heat affected zone).

© 2022 The Authors. Published by ELSEVIER B.V.

This is an open access article under the CC BY-NC-ND license (https://creativecommons.org/licenses/by-nc-nd/4.0)

Peer-review under responsibility of the international review committee of the 12th CIRP Conference on Photonic Technologies [LANE 2022]

Keywords: numerical simulation; radiation hydrodynamics code; ultrafast laser ablation; aluminum thin film; ablation depth

1. Introduction

High performance laser thin film scribing techniques have applications in numerous advanced technology areas including scribing of thin film solar cells and smart window glass, patterning of flexible electronics, micromachining of microelectromechanical systems and light emitting diodes, etc. ultrafast laser ablation has been a subject of extensive study over the years which has the potential to be a high performance scribing technique capable of producing narrow, straight walled cuts with little imparted surface damage. To optimize ultrafast laser scribing processes and develop new techniques, a fundamental understanding of the ablation mechanisms is needed. Because of the complex phenomena involved in the process, various numerical methods have been utilized to shed lights on the underlying physics in ultrafast laser interaction with thin film materials. Two-temperature model (TTM) is one of the early methods used to account for the nonequilibrium thermal state between electrons and lattice at the onset of laser

irradiation, and it was developed as a more practical tool for predicting ablation depth for ultrashort pulse lasers [1]. Molecular dynamics (MD) simulations have been successful in revealing complex phenomena in laser ablation at the atomic level including melting and resolidification, spallation, phase explosion, and material ejection [2,3]. Hydrodynamics simulations provide a comprehensive treatment of laser absorption by the electrons and subsequent events including ionization, energy transfer to the lattice, melting, ablation, and shock wave propagation [4]. Moreover, several hybrid methods have been developed to combine two existing methods for a more complete treatment of the process physics. One commonly used approach is to combine TTM and MD, where laser absorption by electrons and electron-lattice coupling is treated using TTM and lattice dynamics leading to ablation is dealt with using MD simulation [5-7]. TTM has also been coupled with commercial package like COMSOL Multiphysics to simulate laser ablation of metal thin films [8,9]. Over the years simulations have not only enabled visualization of the complex microscopic processes in play during ultrafast laser ablation of thin film materials but also helped the development and optimization of new processes such as double pulse ablation [10] and backside ablation [11]. Because of the different numerical methods used and assumptions made, simulation predictions do not always agree with each other. For example, when simulating femtosecond laser double pulse ablation of aluminum film on glass, a minimum vaporization threshold was identified at delay time of 5-10 ps using TTM [12] while a nearly constant ablation threshold was seen for <10 ps time delays [13]. Therefore, more research is needed in this area, especially for more complicated irradiation schemes. In this paper, ultrafast laser ablation of aluminum thin film on silicon is simulated using a radiation hydrodynamics code, HYADES [14]. The purpose is to study the microscopic mechanisms that are responsible for material ablation, verify the numerical model, and explore the impact of various irradiation schemes on ablation depth in the future.

2. Modeling and simulation procedure

Modeling and simulation of laser-matter interaction with aluminum thin film on silicon substrate is conducted using a 1D radiation hydrodynamics code, known as HYADES. Aluminum is selected as the material in this study because of its well-established material properties and known equation of state. Various physical processes at the microscopic/atomic level during laser-matter interaction including laser deposition, ionization, thermal energy transport, and hydrodynamics motion are considered in the model.

The sample is a 1×1 cm² square shape with a 300 nm thick aluminum film on a 10 µm thick silicon substrate. The mesh points and zones (spatial extent between adjacent mesh points) in the depth direction are shown in Fig. 1. For the aluminum film, a non-uniform mesh starts at Node 1 and gradually increases by a factor of 1.05 to end with Node 101. For the silicon substrate, a uniform mesh of 101 nodes with 100 nm between adjacent nodes is used. Besides the mesh points, a total of 200 zones are defined as shown in the figure because some quantities such as material density and pressure are defined at the zone centers. The sample is surrounded by vacuum. Linearly polarized plane-wave laser pulses irradiate the sample from the left side at normal incidence. The laser pulse follows a Gaussian temporal profile with the power given in Eq (1) as a function of time, where P_{peak} is the peak laser power and $\boldsymbol{\tau}$ is the FWHM pulse duration (full-width at half-maximum). The optical and material properties for aluminum and silicon are given in Table 1.

$$P = P_{peak} e^{\left[-4ln2\left(\frac{t}{\tau}\right)^2\right]} \tag{1}$$

Table 1 Complex refractive indices for aluminum and silicon

Table 1 Complex refractive indices for artifiliting and sincon						
	λ=1030 nm		Thermal	Maltina	Ch com/vi al d	
	n'	n"	conductivity (W/m·K)	Melting model	Shear/yield model	
Aluminum [14, 16]	2.767	8.354	218	Lindemann	Steinberg- Guinan	
Silicon [14,17]	3.562	2.5×10 ⁻⁴	148	N/A	N/A	

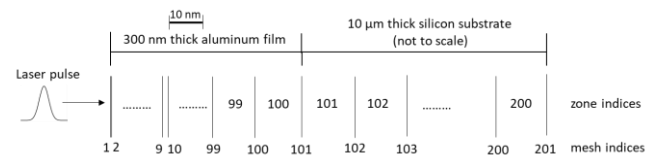


Fig. 1 Illustration of the 1D model for the sample made of aluminum film on a silicon substrate including mesh and zone indices. A laser pulse irradiates the sample from the left.

The HYADES code solves a system of equations including the conservation equations of mass, momentum and energy and a constitutive equation that relates the pressure and specific energy as a function of temperature and density (e.g., equation of state) [15]. The equation of state (EOS) for aluminum and silicon are based on the EOS tables provided in the HYADES User's Guide [14], which are assembled from different sources. The ionization model used in this study is the generalized Thomas-Fermi model of the atom based on Fermi-Dirac statistics, which includes degeneracy effects. Energy transported by the electrons and ions is modeled by flux limited diffusion. The coupling between the electron and ion fluids are through Coulomb collisions. The temperature of each species is computed based on Fourier's law. The hydrodynamics motion of the material is solved using the law of conservation of momentum to determine the velocity and position of the mesh points.

The simulation conditions for single pulse laser irradiation are shown in Table 2. The purpose is to study the effects of laser fluence and pulse duration on ablation depth. Eight fluence values are selected for the pulse duration of 1 ps. Six pulse durations are selected at each of the two laser fluences, 2.49 and 3.12 J/cm². The wavelength, spot size, and light polarization state are fixed.

Table 2 Simulation conditions for single pulse irradiation

Laser parameters	Values		
Fluence, F (J/cm ²)	0.62, 1.25,1.87, 2.49, 3.12, 6.24, 9.35, 12.47		
Pulse duration, τ (ps)	0.184, 0.5, 1, 2, 5, 10		

3. Laser ablation experiments

The setup for the laser ablation experiments is schematically shown in Fig. 2. A femtosecond laser with pulse durations ranging from hundreds of fs to >10 ps is used in the experiments. Pulse energy is adjusted by a half-wave plate and a cube polarizer. A focusing lens (LA1908-B Plano-convex lens from Thorlabs) is used to concentrate the pulse energy to a focal spot on the sample surface. The input beam size is 6.5 mm and the focal spot size is about 100 μ m. The sample is mounted on a motorized xyz stage controlled by a computer. Surface ablation is realized through single shot irradiation with motion control so that each laser shot is fired on a fresh spot on the sample.

For the purpose of model validation, the conditions for the laser ablation experiments are the same as those for the numerical simulation. The laser ablation sites are examined using a 3D optical profiler and the average ablation depth for each crater is extracted.

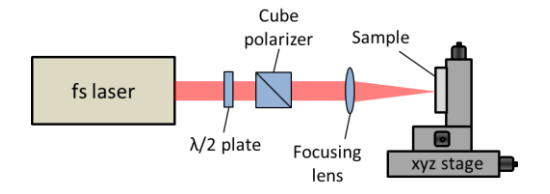


Fig. 2 Schematic of laser ablation experimental setup and (b) laser scan pattern.

4. Results and discussion

Each simulation begins with the input of a single laser pulse and runs continuously until it reaches 1 ns. At the end of the simulation, thermal vaporization should have been initiated and materials leaving the surface are considered ablated. The simulation produces an extensive number of quantities that describe the physical state of the material at its mesh points and zones in time and space. Mass density distribution at the end of each simulation is used to identify the ejected materials, from which the ablation depth is obtained. The results for the aluminum thin film instead of the entire sample (e.g., film plus substrate) are described in the following because the focus is on the response of the aluminum film to laser irradiation in this study. In fact, the substrate is not much disturbed for the laser conditions used in the simulations.

Fig. 3 shows the mass density against the mesh index at 1 ns after laser irradiation for three different conditions. A sharp change in the mass density denotes the boundary between the ejected material and that remains on the sample. Fig. 3 (a) and (b) show the simulation results for the pulse duration of 5 and 1 ps, respectively, with the laser fluence fixed at 2.49 J/cm². It seems that pulse duration has little effect on ablation depth in that the deepest element ejected is the 47th and 51st for the two pulse durations, corresponding to 19 nm and 24 nm, respectively. At 1 ns, the ejected materials are still very close to the surface (up to tens of microns above the surface) and continue to move away from the surface, as confirmed by the mesh positions and velocity vectors (not shown here). Since both pulse durations fall in the ultrafast regime, the ablation mechanism should be similar, and so is the expected ablation depth. Fig. 3(c) shows mass density profile for the fluence of 6.24 J/cm² and the pulse duration of 1 ps. Comparing with Fig. 3(b), it can be seen that the ablation depth is increased to the 62nd element (about 43 nm deep into the surface) as the fluence is 2.5 times higher. The top surface element has already moved to more than 70 µm above the surface.

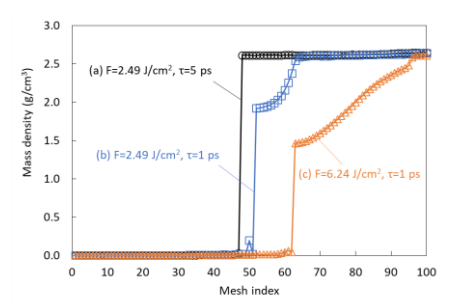


Fig. 3 Mass density of the aluminum thin film at 1 ns after laser irradiation: (a) F=2.49 J/cm² and τ =5 ps, (b) F=2.49 J/cm² and τ =1 ps, and (c) F=6.24 J/cm² and τ =1 ps.

Fig. 4 shows the cross sectional profile and optical image of one ablated spot for illustration purpose. A shallow crater is formed after the laser shot in this case. A general observation indicates two common features seen under different conditions. First, a ridge is formed at the circular boundary of the ablation spot, which may be attributed to plastic flow with subsequent fracturing of the boundary material while resisting the pull-up force by the ejected material. Second, the crater bottom is not flat, which is mainly caused by the Gaussian intensity profile of the laser beam. The bottom is also not very smooth, which indicates the complex microscopic dynamics operating during laser ablation.

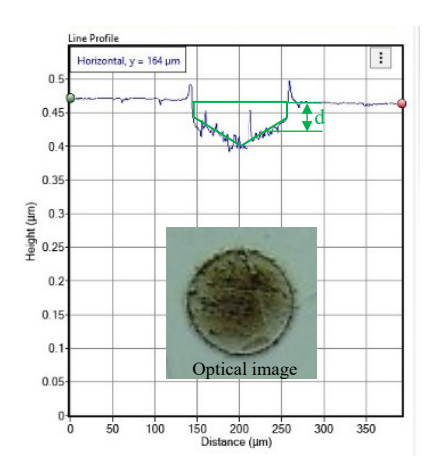


Fig. 4 Cross sectional profile of laser ablated spot: τ=184 fs and F=6.24 J/cm². Inset: optical image of the same spot.

To validate the numerical simulation, model predications and the corresponding experimental results for the ablation depth under various conditions are compared. It should be pointed out that the simulation is one dimensional (in the depth direction) and the experiment is two dimensional (in the depth and radial direction). However, because the laser beam spot size is more than 100 times larger than the ablation depth, the laser ablation experiment can be approximated as a onedimensional case with a gradient fluence decreasing from the beam center radially outward. Therefore, an average ablation depth is estimated for a crater with a non-flat bottom from the experiments and used in the comparison. As illustrated in Fig. 4, the crater cross section is approximated by the green geometry consisting of straight line segments, and the crater depth thus obtained (d) is considered as a first order estimate. In the future, after gaining enough experience with the 1D code, the authors will extend the simulation to 2D to treat more practical problems.

Fig. 5 shows a comparison between simulation and experimental results for ablation depth as the laser fluence increases while keeping the pulse duration fixed at 1 ps. The overall agreement is very good, especially for the laser fluence of greater than 2 J/cm². Both the simulation and experimental results point to a near linear relationship for the ablation depth when laser fluence exceeds 2.5 J/cm². A nonlinear trend is apparent at the lower laser fluence range, more pronounced for the experimental results. It is noted that there is a relatively large discrepancy at low laser fluence levels between the

simulation and experimental results, for which the cause is unclear at this time. More work is needed to clarify this issue, and one of the things that need to be considered is to include ambient air in the simulation since the experiments are performed in air. Fig. 6 shows the variations of ablation depth with pulse duration at two laser fluence levels, 2.49 and 3.12 J/cm². Again, the overall agreement between the simulation and experimental results is good in terms of the relative magnitude and trend for the ablation depth. A weak linearly decreasing trend for ablation depth beyond 1 ps is seen for both laser fluence levels. The cases for pulses shorter than 1 ps seem to be more complicated. A significant jump in ablation depth occurred in the experiments at the pulse duration of 0.5 ps, and the simulation is able to capture this "anomaly" but with a large gap from the measured data. This behavior needs to be verified both experimentally and in simulations before any conclusions can be drawn for the reasons behind it.

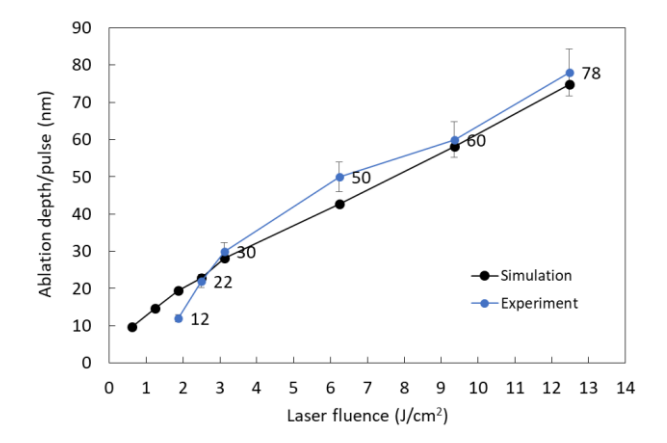


Fig. 5 Variations of laser ablation depth with laser fluence.

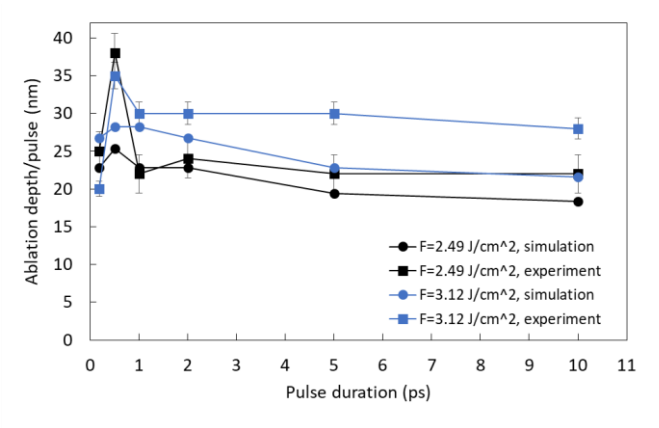


Fig. 6 Variations of laser ablation depth with pulse duration.

5. Conclusions

The HYADES radiation hydrodynamics code is used to simulate laser irradiation of aluminum thin film on silicon substrate. Ablation depth is extracted from the simulation results at 1 ns. Model validation is performed by comparing the simulation and experimental results in terms of ablation depth as a function of laser fluence and pulse duration. A good agreement is reached between the simulation and experiments. The hydrodynamics model is able to capture the linearly

increasing trend of ablation depth with laser fluence for F>2.5 J/cm². Further investigation is needed to verify the model's predictive capability for the lower fluence range. The average prediction error is 12%. Similarly, for the pulse duration, the model is capable of predicting the trend in ablation depth as pulse duration changes, and the average error in magnitude is 19%. In summary, the hydrodynamics model can provide more reliable predictions for laser ablation experiments at large fluences (e.g., >2 J/cm²) and can be used in the future to assist in the design of experiments to explore new laser ablation strategies.

Acknowledgements

Financial support for this work by the National Science Foundation under Grant No. CMMI-1903740 is gratefully acknowledged.

References

- Wu B, Shin YC. A sample model for high fluence ultrashort pulsed laser metal ablation. Applied Surface Science 2007; 253:4079-84.
- [2] Zhigilei LV, Lin Z, Ivanov DS. Atomistic modeling of short pulse laser ablation of metals: connections between melting, spallation, and phase explosion. J. Phys. Chem C 2009; 113: 11892-906.
- [3] Upadhyay AK, Inogamov NA, Rethfeld B, Urbassek HM. Ablation by ultrashort laser pulses: Atomistic and thermodynamic analysis of the processes at the ablation threshold. Physical Review B 2008; 78: 045437.
- [4] Povarnitsyn ME, Itina TE, Sentis M, Khishchenko KV, Levashov PR. Material decomposition mechanisms in femtosecond laser interactions with metals. Physical Review B 2007; 75: 235414.
- [5] Sonntag S, Rogh J, Gaehler F, Trebin HR. Femtosecond laser ablation of aluminum. Applied Surface Science 2009; 255: 9742-44.
- [6] Wu C, Zhigilei L. Microscopic mechanisms of laser spallation and ablation of metal targets from large-scale molecular dynamics simulations. Appl. Phys. A 2014; 114: 11-32.
- [7] Amoruso S, Nedyalkov NN, Wang X, Ausanio G, Bruzzese R, Atanasov PA. Ultrashort pulse laser ablation of gold thin film targets: Theory and experiment. Thin Solid Film 2014; 550: 190-198.
- [8] Sotrop J, Kersch A, Domke M, Heise G, Huber HP. Numerical simulation of ultrafast expansion as the driving mechanism for confined laser ablation with ultrashort laser pulses. Appl. Phys. A 2013; 113: 397-411.
- [9] Gupta PD, O'Connor GM. Comparison of ablation mechanisms at low fluence for ultrashort and short-pulse laser exposure of very thin molybdenum films on glass. Applied Optics 2016; 55: 2117-25.
- [10] Povarnitsyn ME, Itina TE, Levashov PR, Khishchenko KV. Simulation of ultrashort double-pulse laser ablation. Applied Surface Science 2011; 257: 5168-71.
- [11] Rouleau CM, Shih CY, Wu C, Zhigilei LV, Puretzky AA, Geohegan DB. Nanoparticle generation and transport resulting from femtosecond laser ablation of ultrathin metal films: Time-resolved measurements and molecular dynamics simulations. Applied Physics Letters 2014; 104: 193106.
- [12] Olbrich M, Punzel E, Roesch R, Oettking R, Muhsin B, Hoppe H, Horn A. Case study on the ultrafast laser ablation of thin aluminum films: Dependence on laser parameters and film thickness. Appl. Phys. A 2016; 122: 215.
- [13] Kudryashov SI, Samokhvalov AA, Golubev YD, Ivanov DS, Garcia ME, Veiko VP, Rethfeld B, Mikhailovskii VYu. Dynamic all-optical control in ultrashort double-pulse laser ablation. Applied Surface Science 2021; 537: 147940.
- [14] HYADES User's Guide. Cascade Applied Sciences, Inc. 2019.
- [15] Larsen JT, Lane SM. HYADES a plasma hydrodynamics code for dense plasma studies. J. Quant. Spectros. Radiat. Transf. 1994; 51: 179-186.
- [16] https://refractiveindex.info/
- [17] https://www.el-cat.com/silicon-properties.htm